Proceedings of the ASME 2010 3rd Joint US-European Fluids Engineering Summer Meeting and 8th International Conference on Nanochannels, Microchannels, and Minichannels
FEDSM-ICNMM2010
August 1-5, 2010, Montreal, Canada

FEDSM-ICNMM2010-30761

HEAT TRANSFER AND EVAPORATION OF FALLING LIQUID FILMS ON SURFACES WITH ADVANCED THREE-DIMENSIONAL PERIODIC STRUCTURES: EXPERIMENTS AND NUMERICAL SIMULATIONS

Karsten Löffler[1], Hongyi Yu[1], Steffen Hardt[2], Tatiana Gambaryan-Roisman[1,2] and Peter Stephan[1,2]

[1]Institute for Technical Thermodynamics, Technische Universität Darmstadt,
Petersenstr. 30, Darmstadt, 64287, Germany

[2]Center of Smart Interfaces, Technische Universität Darmstadt,
Petersenstr. 32, Darmstadt, 64287, Germany

ABSTRACT

Thin liquid films are widely used in many technological applications. Heat and mass transfer in falling liquid films can be controlled and enhanced by using walls with advanced three-dimensional topographies that influence the film hydrodynamics, stability and wavy pattern or promote evaporation in a very thin film region. Furthermore, capillary suction on structured surfaces leads to a significant increase of the critical heat flux.

In this work, heat transfer in laminar falling water films on heated plates with herringbone structure and with meandering grooves has been studied experimentally for different heat fluxes (up to 24 kW/m²), inclination angles and flow rates under reduced pressure, so that evaporation has a significant impact on heat transfer. The flow patterns and temperature gradients on the liquid-gas interface are visualized by high-speed infrared thermography. The wall temperature distribution is measured with thermocouples. The experimental data are compared with the results of numerical simulations.

The predicted effect of micro region evaporation on heat transfer has been confirmed experimentally for the first time for partially wetting films on a plate with meandering grooves. This effect manifests itself in a significant decrease of the local wall temperature after the film rupture and consequent transition from a continuous film flow to rivulet flow regime.

NOMENCLATURE

p	pressure, bar
q	heat flux, W/m^2
Re	Reynolds number
T	temperature, °C
u	velocity in streamwise direction, m/s
x	streamwise direction, distance from film inlet, m
y	spanwise direction, m
Γ	mass flow rate per channel width, kg/(m s)
β	plate inclination angle
μ	dynamic viscosity, kg/(m s)

Subscripts

w	wall

INTRODUCTION

Thin liquid films are characterized by large surface-to-volume ratio. The major advantages of falling liquid films for heat transfer applications are high heat and mass transfer rates and short contact time between the liquid and the solid wall. Falling liquid films are widely used in industrial apparatuses and processes which include cooling, evaporation, condensation and absorption. Understanding of transport processes in liquid films is very important for designing industrial apparatuses and for determination of the process parameters.

Hydrodynamics and heat transfer in falling liquid films have been a topic of numerous investigations over several decades [18], [27], [9], [3]. Heat and mass transfer in falling liquid films is determined by the film thickness distribution, the velocity field inside the film and the thermal conditions at the liquid-gas interface [24], [25], [1], [2], [19], [20]. In most cases the heat transfer coefficient varies along the flow direction.

Smooth falling films are unstable to long-wave disturbances [5], [29], [30]. This instability leads to development of waves at the liquid-gas interface. The hydrodynamics of the wavy films depend on the film Reynolds number, on the plate inclination angle, on the distance from the liquid inlet and on the mode of the disturbance [1], [3].

One of the limitations of thin falling liquid film application on heated walls is film rupture which leads to wall dryout. The film rupture mechanisms include poor wettability, thermo-capillarity and vapor recoil [14], [6], [23], [7]. The wall heat flux corresponding to dryout increases with increasing of the film Reynolds number [31]. The film dryout generally dramatically deteriorates the heat transfer and may lead to the apparatus damage. However, it has been shown that under certain conditions (for example, in the case of local heating) the film dryout leads to formation of several rivulets along the flow direction. This flow arrangement may lead to intensification of the heat transfer in comparison to the continuous film [7]. This intensification can be attributed to the evaporation of the ultra-thin liquid film in the vicinity of apparent contact lines separating the rivulets from the dry wall [26].

The transport processes in falling liquid films can be further intensified by using (micro-) structured walls [11], [12], [15]. The wall topography affects the heat transfer in falling liquid films through the promotion of the rivulet flow regime characterized by intensive evaporation [12], [17], creation of the vortex flow patterns [28] and development of Marangoni convection [4]. Moreover, the wall topography modifies the wave development on the liquid-gas interface [13]. It has been predicted theoretically and confirmed by experimental investigations that longitudinal grooves stabilize the film flow [12], [16], [21].

In the present paper the flow patterns and heat transfer in falling liquid films on meandering and zigzag mini-grooves are investigated experimentally and compared with numerical simulations. The flow patterns and temperature distribution determined from numerical simulations helps to understand the liquid motion and heat transfer on the grooved plates.

EXPERIMENTAL SETUP AND MEASUREMENT PROCEDURE

The experimental facility for investigation of the falling films is schematically depicted in Fig. 1. The test channel is made of stainless steel and equipped with exchangeable electrically heated plates. The inclination angle of the plate against horizontal can be varied from 0° to 90°. The experiments have been performed with two brass plates. The first has meandering (sinusoidal) mini-grooves along the main flow direction (groove depth 0.3mm, width 0.5 mm) with a period of the sinusoidal path of 20 mm and an amplitude of 3 mm. The other has zigzag mini-grooves transverse to the flow direction with the depth of 0.15 mm and the width of 0.3 mm (herringbone structure). The geometry of the structured plates is illustrated in Fig. 2.

All tests have been carried out at an absolute pressure of $p = 100$ mbar. The test liquid (deionized water) is supplied from the storage tank to a small chamber at the top of the test channel by a gear pump. A small adjustable slot in the chamber acts as film distributor. After flowing down the test section the water flows back to the tank, so that a closed liquid circulation loop is maintained. The flow rate is adjusted by a needle valve via a bypass. A membrane pump is used to set the operating pressure and remove vapor from the test channel. The vapor is condensed in a plate heat exchanger and flows back to the storage tank.

The water inlet temperature has been kept constant at 30 °C by a thermostat. The area of the metal plate of 145 x 575 mm² below the film distributor has been heated uniformly by an electrical heating foil.

The wall temperature has been measured by thermocouples at 25 locations which are positioned in bore holes at a distance of 1 mm from the metal surface of the plate (at the crest of the structure). The surface temperature distribution of the liquid film has been measured by infrared thermography at three different positions (image center positioned at distances x = 85 mm, 285 mm and 485 mm from the inlet) through IR-transparent windows made of calcium fluoride. The infrared images have been taken with the Phoenix-MID camera with a frame rate of 323 Hz in the spectral range of 3-5 µm. The field of view (FOV) for the infrared images has been 55 x 63 mm².

The infrared thermography can be used on one hand for qualitative characterization of the flow patterns in the falling film and on the other to evaluate the film surface temperature. Moreover, due to the significant difference in emissivity between the water and the wall material, the infrared thermography is one of the best methods for distinguishing between the wetted and dry portions of the wall.

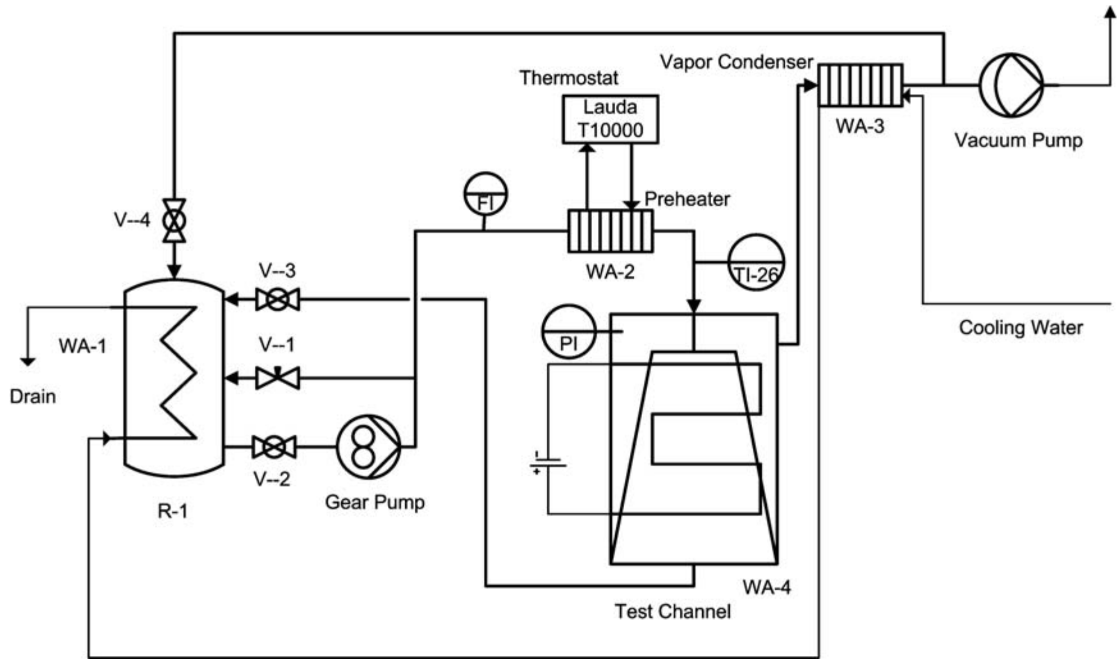

Figure 1. Experimental setup

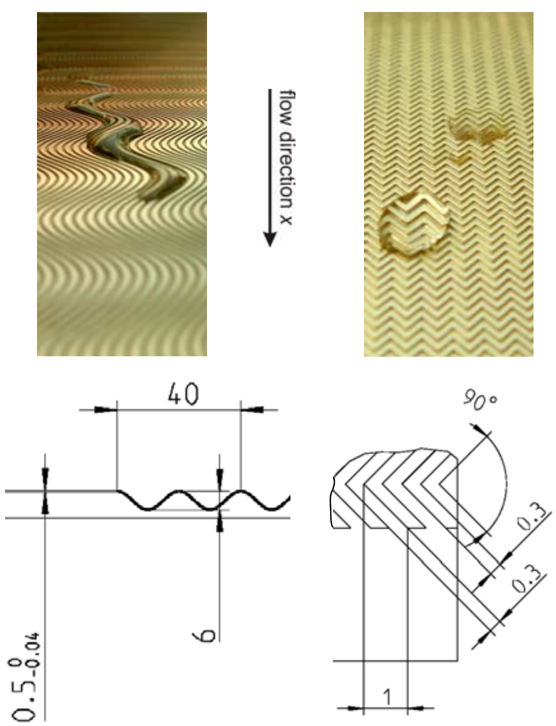

(a) (b)

Figure 2. Structured plates: (a) plate with meandering mini-grooves; (b) plate with zigzag mini-grooves

For the evaluation of film surface temperatures a calibration has been carried out at the first window on an unstructured brass plate. Water has been supplied at different temperatures at a constant mass flow rate of 100 kg/h at an inclination angle of 20°. The inlet temperatures have been measured with a thermocouple closely before the film distributor. As the film surface at this place and for these parameters is rather smooth and heat losses are very low, an isothermal film surface is a reasonable assumption in this region. An average of fifty infrared frames has been taken and the measured temperatures have been correlated with the forth root of the resulting radiation intensities for each pixel. In case of strong evaporation the obtained surface temperatures are very close to the saturation temperature, which is an additional validation of the calibration procedure.
From the calibration procedure and the resulting temperatures, the overall accuracy of the wall temperature measurement can be estimated to +/- 0.5 K and the liquid surface temperature to +/- 1 K.

The measurements have been taken at different mass flow rates, plate inclination angles and heat fluxes.

NUMERICAL SIMULATION

In order to get further insight into the flow and heat transfer on structured plates, a numerical simulation has been carried out on a representative part of the geometry with the commercial CFD-package Fluent to solve the continuity, Navier-Stokes and energy equations with a finite-volume approach. The standard PISO algorithm has been used.

A length of 45 mm in flow direction has been resolved for the meandering mini-grooves with an unstructured mesh of tetrahedral and prismatic elements and 300 mm for the zigzag mini-grooves with a structured mesh of hexahedral elements.

It is assumed that the flow is stationary, laminar and hydrodynamically fully developed and that the liquid-gas interface is flat. The resulting film thickness over the respective parts of the structured plates has been derived iteratively from the numerical simulations. A constant heat flux boundary condition has been applied at the wall and a convective boundary condition at the liquid-gas interface.

RESULTS AND DISCUSSION

Plate with meandering grooves

Figure 3 shows the wall temperature distribution in streamwise direction for various heat fluxes at an inclination angle of $\beta = 45°$ of the plate with meandering grooves at Re = 144. Herein the Reynolds number Re is defined as $Re = \Gamma / \mu$, where Γ is the mass flow rate per channel width and μ is the dynamic viscosity of the liquid at inlet conditions. For heat fluxes up to 12 kW/m² the temperatures are linearly rising along the flow direction over almost the whole length of the plate. This behavior corresponds to a fully developed temperature field at adiabatic fluid gas-interface conditions [21]. At higher heat fluxes, however, the temperature profiles are characterized by a steep temperature rise near the film inlet. After a few centimeters the wall temperatures reach an almost constant level. This behavior corresponds to a fully developed temperature profile for high Biot numbers at the liquid-gas interface, i.e. significant heat transfer from the liquid to the gas phase [22]. The high heat transfer rate between the liquid and the gas is an indication of the importance of evaporation. Hence, at certain conditions moderate increase of heat flux leads to a significant jump in the wall temperature over a wide region of the plate.

On an unstructured plate however, this state cannot be reached as for $\beta = 45°$and Re = 144 the film is ruptured in a large area at q = 7.2 kW/m². In that case strong evaporation has not set in yet and the wall temperature is rising steeply so that the heating has to be stopped to prevent material damage.

How does the significant change of Biot number affect the fluid flow and the temperature distribution at the liquid-gas interface? Figure 4 shows the corresponding liquid surface temperature distribution for q = 12 kW/m², where the center of the image is positioned at x = 285 mm. The wave pattern is rather complex and significant temperature increase along the flow direction (from upper to lower regions of the image) is seen.

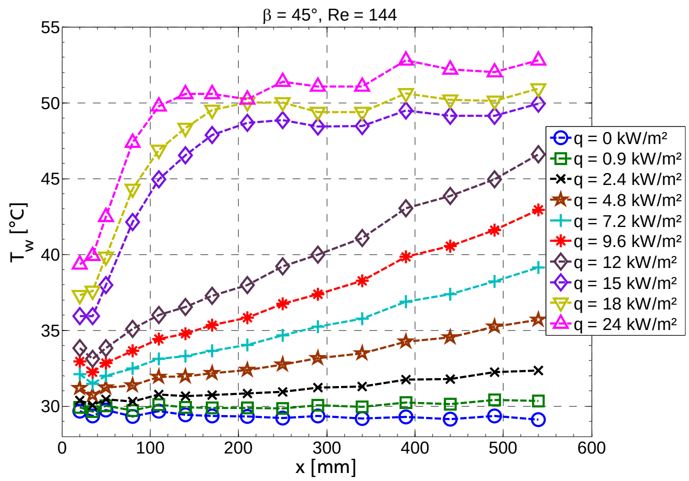

Figure 3. Wall temperature distribution in streamwise direction x for Re = 144, $\beta = 45°$ on plate with meandering grooves

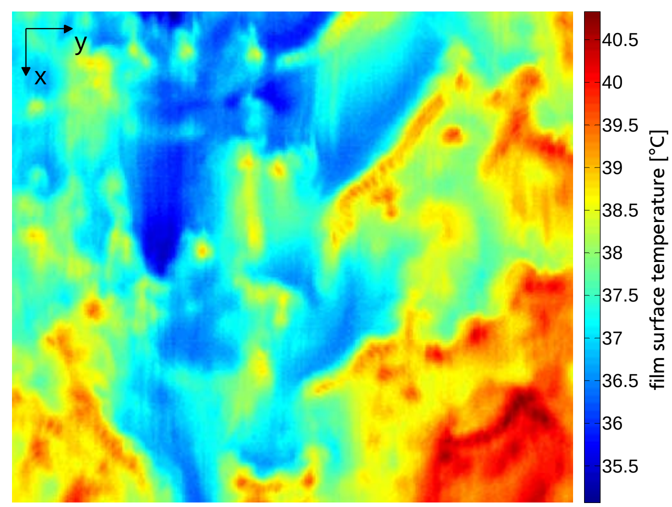

Figure 4. Film surface temperature for Re = 144, $\beta = 45°$, x = 285 mm and q = 12 kW/m² on plate with meandering grooves

The increase in wall temperature for q = 15 kW/m² in comparison to q = 12 kW/m² also manifests itself in an increase in liquid-gas interface temperature, see Figure 5. The temperature is uniform over a large interface area and close to saturation temperature which is 45.8°C at p = 100 mbar. It can be concluded that in this case the major heat transfer mechanism between the liquid and gas is evaporation. The thermally developed regime corresponds to constant temperatures at the wall and at the liquid-gas interface.

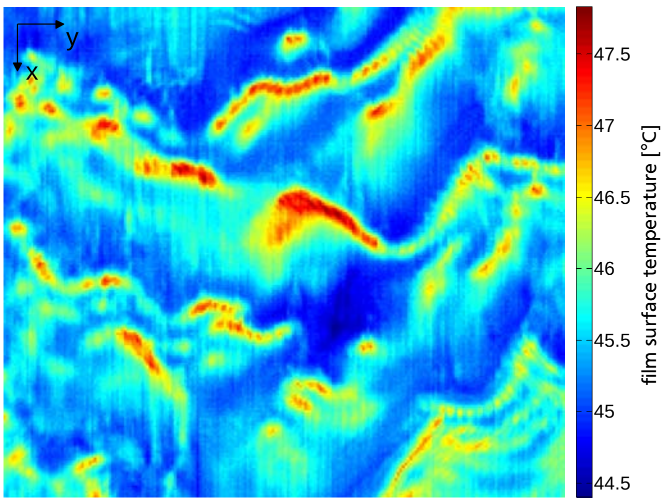

Figure 5. Film surface temperature for Re = 144, $\beta = 45°$, x = 285 mm and q = 15 kW/m² on plate with meandering grooves

The non-uniformity of the temperature distribution seen in Fig. 5 is attributable to the wavy motion of the film. Horseshoe-like waves can be discerned which are preceded by small hot zones. These correspond to capillary wave troughs where vortices transport hot, supersaturated liquid to the surface. The existence of these vortices has been found and explained by Dietze *et al.* [10]. Similar transition phenomena can be observed for other inclination angles and Reynolds numbers for other heat fluxes.

The temperature distribution in the plate with meandering grooves for $\beta = 90°$ and Re = 48 is shown in Fig. 6. The wall temperature distribution at these condition is qualitatively similar to that for $\beta = 45°$ and Re = 144 while the thermal entrance length is shorter.

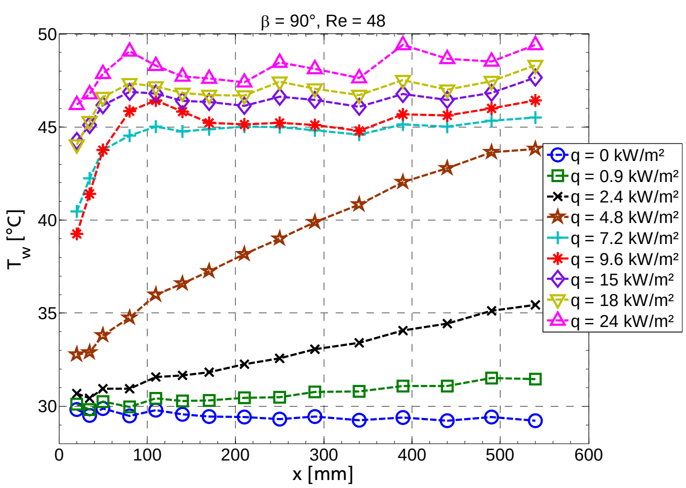

Figure 6. Wall temperature distribution in streamwise direction x for Re = 48, $\beta = 90°$ on plate with meandering grooves

The corresponding liquid-gas interface temperature for q = 4.8 kW/m² is shown in Figure 7. Colder liquid can be seen at the left side while the temperature is increasing to the bottom and right side. Thermocouple positions have been drawn as black circles at x = 290 mm and will be referred to later. Again horseshoe-like waves with preceding capillary waves are observed.

At further increase of heat flux, not only saturation is reached but also partial film rupture occurs on the crests of the plate structure. However the wall temperature is not rising further, since the grooves are still partially filled with water and strong evaporation takes place. Figure 8 shows the resulting pattern at q = 9.6 kW/m². The three thermocouple positions correspond to the transversal positions y = 51.5 mm, 72.5 mm (plate center) and 93.5 mm in Figure 9. The two left thermocouples are in or near regions where only partial wetting of the plate is observed. These regions are characterized by a large density of three-phase contact lines separating the wetted and unwetted areas of the plate. Surprisingly the wall temperature in these partial wetted zones is lower than in the fully wetted zones as seen from Figure 9. A temperature drop from the fully wetted to the partially wetted zone can be clearly seen in this area. This phenomenon is not observed at q = 4.8 kW/m², where the metal surface is fully covered. This is a proof of the strong cooling effect of evaporation in the vicinity of three-phase contact lines, where the film is extremely thin. This effect has been theoretically predicted for falling films on grooved walls by Gambaryan-Roisman and Stephan [12].

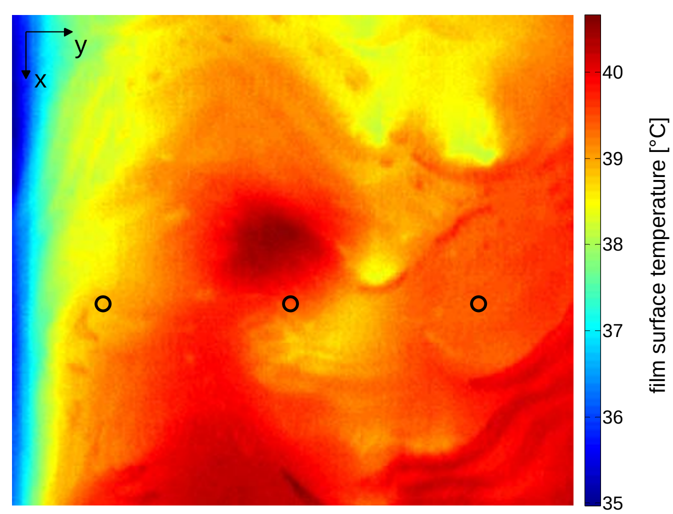

Figure 7. Film surface temperature for Re = 48, $\beta = 90°$, x = 285 mm and q = 4.8 kW/m² on plate with meandering grooves, black circles correspond to thermocouple positions

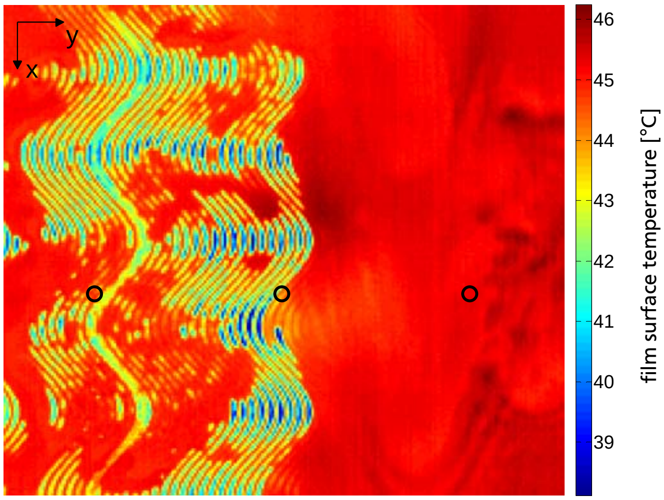

Figure 8. Film surface temperature for Re = 48, $\beta = 90°$, x = 285 mm and q = 9.6 kW/m² on plate with meandering grooves, black circles correspond to thermocouple positions

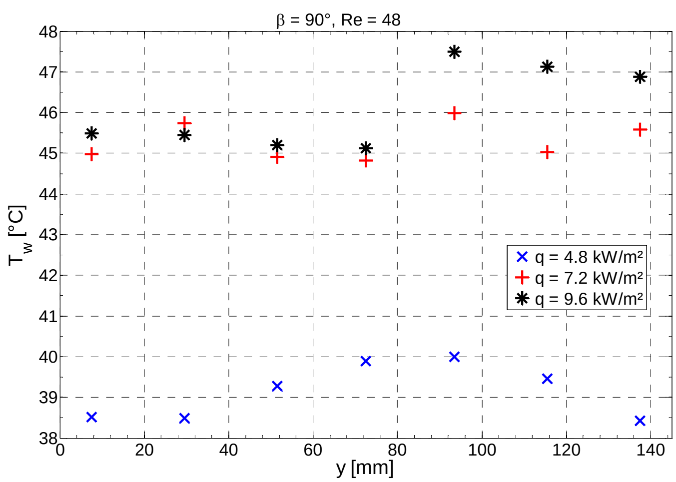

Figure 9. Wall temperature distribution at x = 290 mm in spanwise direction y for Re = 48, $\beta = 90°$ on plate with meandering grooves

Plate with zigzag grooves

An example of the temperature distribution at the liquid-gas interface over the plate with zigzag grooves is given in Figure 10 at x = 85 mm. The temperature profile is characterized by periodic stripes of warmer and colder liquid. Their width corresponds to half the width of a herringbone. At the lower left corner of the image, the stripes are distorted by onset of wavy motion of the liquid interface. The circular distortion comes from reflections of the infrared window, since the emission from the liquid interface in this temperature range close to the film distributor is not significantly larger than the reflected radiation.

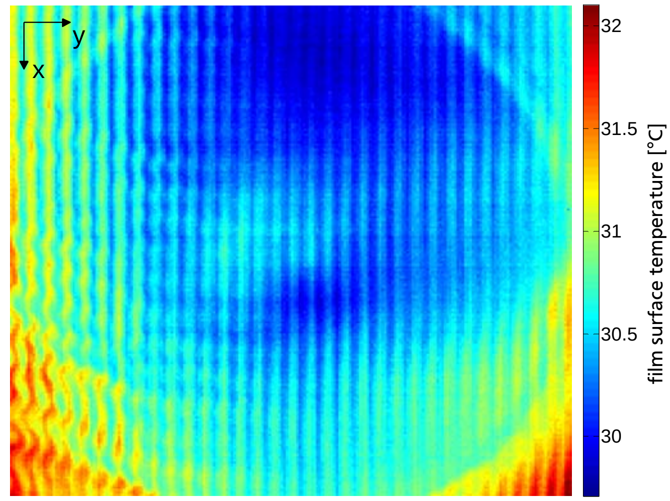

Figure 10. Film surface temperature for Re = 144, $\beta = 20°$, x = 85 mm and q = 9.6 kW/m² on plate with zigzag grooves

To explain this temperature distribution, consider first a computed velocity distribution in a falling film flowing over a plate with zigzag grooves (Figure 11).

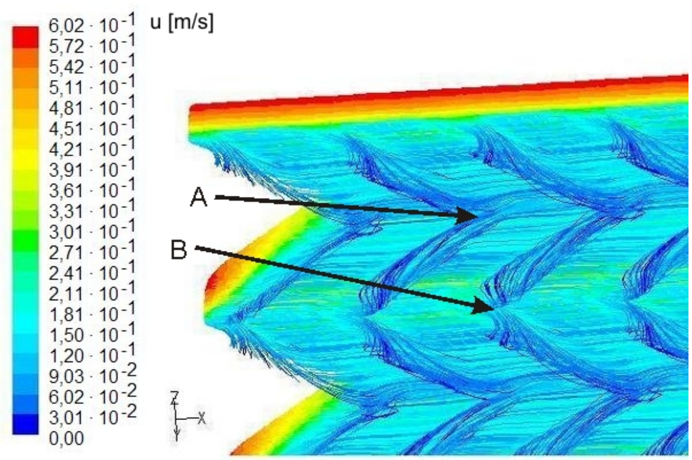

Figure 11. Streamlines of liquid flow on zigzag geometry for Re = 115, $\beta = 90°$, colors represent velocity magnitude in m/s

The flow is channeled in the grooves of the herringbone leading to lower flow velocities at positions where the tip of the groove path is facing downstream (position A) and faster velocity where the tip of the groove path is facing upstream (position B). Due to the different residence times of the liquid at the different positions on the herringbone pattern, the liquid is heating up faster in zones of smaller velocity. The resulting temperature distribution at the liquid-gas interface is illustrated in Figure 12. It is evident that the temperature field is periodic in transverse direction, which is in a qualitative agreement with Fig. 10. Although other parameter values have been used in the computations, the results are qualitatively similar and can be used to explain the experimental findings.

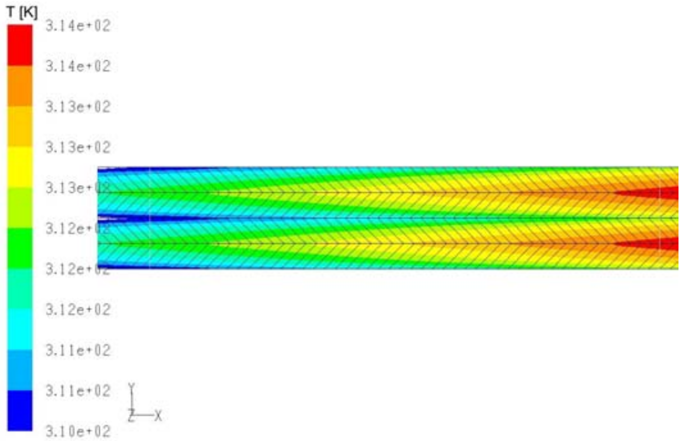

Figure 12. Computed liquid–gas interface temperature distribution in falling film on a plate with zigzag grooves for Re = 38, β = 45°and q = 15 kW/m²

CONCLUSIONS

Heat transfer and evaporation of falling liquid films on plates with three-dimensional mini grooves have been studied experimentally. Significantly higher heat fluxes than on smooth plates can be obtained on these structures.

A noticeable change in temperature profile and flow pattern can be observed when saturation condition is reached at the liquid-gas interface. In case of partial film rupture on a plate with meandering grooves the strong cooling effect of micro region evaporation manifests itself by significant enhancement of the cooling performance.

In the case of a plate with herringbone pattern the liquid-gas interface is characterized by a spatially-periodical temperature distribution, which could be explained by a numerical simulation.

The present study emphasizes the possibilities of improving and controlling falling liquid film flow, heat and mass transfer by optimizing the combination of advanced wall structures and the flow parameters.

ACKNOWLEDGMENTS

The authors wish to acknowledge the support of the German Science Foundation, DFG, through the Emmy Noether Program. Special thanks to the students Marc Arnold, Tobias Benker and Teresa Warmuth who carried out the experiments and simulations during their bachelor theses.

REFERENCES

[1] Adomeit, P. and Renz, U., 2000, Hydrodynamics of Three-Dimensional Waves in Laminar Falling Films, *Int. J. Multiphase Flow*, Vol. 26, pp. 1183-1208.

[2] Al-Sibai, F., Leefken, A., Renz, U., 2002, Local and Instantaneous Distribution of Heat Transfer Rates through Wavy Films, *Int. J. Therm. Sci.* Vol. 41, pp. 658-663.

[3] Alekseenko, S.V., Nakoryakov, V.E., Pokusaev, B.G., 1994, *Wave Flow of Liquid Films*, Begell House, New York, USA.

[4] Alexeev, A.; Gambaryan-Roisman, T. & Stephan, P., 2005, Marangoni Convection and Heat Transfer in Thin Liquid Films on Heated Walls with Topography: Experiments and Numerical Study, *Phys. Fluids* **17**, 062106-1 - 062106-13.

[5] Benjamin, T.B., 1957, Wave Formation in Laminar Flow down an Inclined Plane, *J. Fluid Mech.*, Vol. 2, pp. 554-574.

[6] Bohn, M.S. and Davis, S.H., 1993, Thermocapillary Breakdown of Falling Liquid Films at High Reynolds Numbers, *Int. J. Heat Mass Transfer*, Vol. 36, No 7, pp. 1875-1881.

[7] Chinnov, E.A., Sharina, I.A., Kabov, O.A., 2004, Intensification of heat transfer in a downward liquid film flow, *J. of Applied Mechanics and Technical Physics*, Vol. 45, No 5, pp. 705-711.

[8] Chinnov, E.A., Kabov, O.A., Zhukovskaya, O.V., Sharina, I.A., 2006, Heat Transfer in a Subcooled Evaporating Liquid Films, *High Temperature*, Vol. 44, pp. 898-907.

[9] Chun, K.R. and Seban, R.A., 1971, Heat Transfer of Evaporating Liquid Films, *ASME J. Heat Transfer*, Vol. 93, pp. 391-396.

[10] Dietze, G. F.; Leefken, A., Kneer, R., 2008, Investigation of the Backflow Phenomenon in Falling Liquid Films, *J. Fluid Mech.* Vol. 595, pp. 435-459.

[11] Fujita, Y., 1998, Boiling and Evaporation of Falling Film on Horizontal Tubes and its Enhancement on Grooved Tubes, pp. 325-346 in *Heat Transfer Enhancement of Heat Exchangers*, ed. by S. Kakac, A.E. F. Mayinger, H. Yuncu, Kluwer Academic Publishers, Dordrecht, The Netherlands.

[12] Gambaryan-Roisman, T. and Stephan, P., 2003, Analysis of Falling Film Evaporation on Grooved Surfaces, *Int. J. Enhanc. Heat Transfer*, Vol. 10, No 4, pp. 445-457.

[13] Gambaryan-Roisman, T., Yu, H., Löffler, K., Stephan, P., 2009, Long-Wave and Integral Boundary Layer Analysis of Falling Film Flow on Walls with Three-Dimensional Periodic Structures, *Proc. 7th Intern. Conf. on Nano-, Micro- and Minichannels*, ICNMM2009-82115, June 22-24, Pohang, South Korea.

[14] Hartley, D.E. and Murgatroyd, W., 1964, Criteria for the Break-Up of Thin Liquid Layers Flowing Isothermally over Solid Surfaces, *Int. J. heat Mass Transfer*, Vol. 7, pp. 1003-1015.

[15] Helbig, K., Alexeev, A., Gambaryan-Roisman, T., Stephan, P., 2005, Evaporating of Falling and Shear-Driven Thin Films on Smooth and Grooved Surfaces, *Flow, Turbulence and Combustion*, Vol. 75, pp. 85-104.

[16] Helbig, K., Nasarek, R., Gambaryan-Roisman, T., Stephan, P., 2009, Effect of Longitudinal Minigrooves on Flow Stability and Wave Characteristics of Falling Liquid Films, *J. Heat Transfer*, Vol. 131, pp. 011601-1-011601-8.

[17] Kabov, Yu.O., Alexeev, A., Gambaryan-Roisman, T., Stephan, P., 2006, Marangoni-Induced Deformation and Rupture of a Liquid Film on a Heated Microstructured Wall, *Phys. Fluids*, Vol. 18, 012104.

[18] Kapitza, P.L., 1948, *Zh. Eksp. Tero, Fiz.* Vol. 18, p.19.

[19] Lel, V.V., Al-Sibai, F., Leefken, A., Renz, U., 2005, Local Thickness and Wave Velocity Measurement of Wavy Films with a Chromatic Confocal Imaging Method and a Fluorescence Intensity Technique, *Exp. In Fluids*, Vol. 39, pp. 856-864.

[20] Lel, V.V., Stadler, H., Pavlenko, A., Kneer, R., 2007, Evolution of Metastable Quasi-Regular Structures in Heated Wavy Liquid Films, *Heat and Mass transfer*, Vol. 43, No 11, pp. 1121-1132.

[21] Löffler, K., Gambaryan-Roisman, T., Stephan, P., 2007, Wave Patterns in Thin Films Flowing down Inclined Smooth and Structured Plates, *Proc. 6th International Conference on Multiphase Flow, ICMF* 2007, July 9-13, Leipzig, Germany.

[22] Löffler, K., Yu, H., Gambaryan-Roisman, T., Stephan, P., 2008, Flow Patterns and Heat Transfer in Thin Liquid Films on Walls with Straight, Meandering and Zigzag Mini-grooves, *Proc.6th Intern. Conf. on Nanochannels, Microchannels and Minichannels*, ICNMM2008-62318, June 23-25, Darmstadt, Germany.

[23] Oron, A., Davis, S.H., Bankoff, S.G., 1997, Long-Scale Evolution of Thin Liquid Films, *Rev. Mod. Phys.*, Vol. 69, pp. 931-980.

[24] Schmerler, J.A. and Mudawar, I., 1988a, Local Heat Transfer Coefficient in Wavy Free-Falling Turbulent Liquid Films Undergoing Uniform Sensible Heating, *Int. J. Heat Mass Transfer*, Vol. 31, No 1, pp. 67-77.

[25] Schmerler, J.A. and Mudawar, I., 1988b, Local Evaporative Heat Transfer Coefficient in Free-Falling Turbulent Liquid Films, *Int. J. Heat Mass Transfer*, Vol. 31, No 4, pp. 731-742.

[26] Stephan, P. and Busse, C.A., 1992, Analysis of Heat Transfer Coefficient of Grooved Heat Pipe Evaporator Walls, *Int. J. Heat Mass Transfer*, Vol. 35, pp. 383-391.

[27] Telles, A.S. and Dukler, A.E., 1970, Statistical Characteristics of Thin, Vertical, Wavy, Liquid Films, Ind. Eng. Chem. Fundam., Vol. 9, No 3.

[28] Wierschem, A. and Aksel, N., 2004, Influence of Inertia on Eddies Created in Films Creeping over Strongly Undulated Surfaces, *Phys. Fluids*, Vol. 16, No 12, pp.4566-4574.

[29] Yih, C.-S., 1955, Stability of Parallel Laminar Flow with a Free Surface, *Quart. Appl. Math.*, Vol. 13, pp. 434-439.

[30] Yih, C.-S., 1963, Stability of Liquid Flow down an Inclined Plane, *Phys. Fluids*, Vol. 6, No 3, pp. 321-334.

[31] Yu, H., Löffler, K., Gambaryan-Roisman, T. Stephan, P., 2008, Heat Transfer in Thin Liquid Films Flowing Down Heated Inclined Grooved Plates, *Proc. CHT-08 ICHMT Intern. Symposium on Advances in Computational Heat Transfer*, CHT-08-210, May 11-16, Marrakech, Morocco.